# A General Route for Nanoemulsion Synthesis Using Low-Energy Methods at Constant Temperature

Ankur Gupta,[†][iD] Abu Zayed Md Badruddoza,[†] and Patrick S. Doyle*[iD]

Massachusetts Institute of Technology, E17-504F, 77 Mass Avenue, Cambridge, Massachusetts 02139, United States

S *Supporting Information*

ABSTRACT: The central dogma of nanoemulsion formation using low-energy methods at constant temperature—popularly known as the emulsion inversion point (EIP) method—is that to create O/W nanoemulsions, water should be added to a mixture of an oil and surfactant. Here, we demonstrate that the above order of mixing is not universal and a reverse order of mixing could be superior, depending on the choice of surfactant and liquid phases. We propose a more general methodology to make O/W as well as W/O nanoemulsions by studying the variation of droplet size with the surfactant hydrophilic–lypophilic balance for several model systems. Our analysis shows that surfactant migration from the initial phase to the interface is the critical step for successful nanoemulsion synthesis of both O/W and W/O nanoemulsions. On the basis of our understanding and experimental results, we utilize the reverse order of mixing for two applications: (1) crystallization and formulation of pharmaceutical drugs with faster dissolution rates and (2) synthesis of alginate-based nanogels. The general route provides insights into nanoemulsion formation through low-energy methods and also opens up possibilities that were previously overlooked in the field.
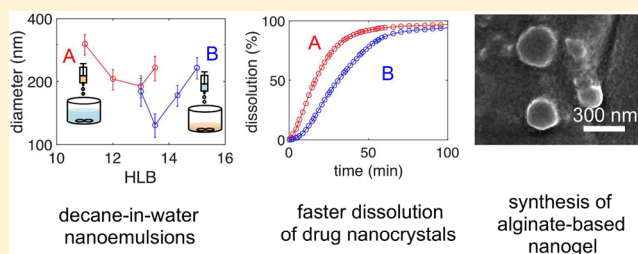
Nanoemulsions are kinetically stable droplets of one liquid phase dispersed in another immiscible phase with sizes on the order of 100 nm, leading to many intriguing properties, such as high surface area, good optical clarity, robust stability, and tunable rheology.[1−6] Nanoemulsions are used to improve the bioavailability of bioactives (drugs, vitamins, nutraceuticals, supplements, etc.),[6−10] to synthesize templated nanoparticles and advanced polymeric materials,[11−13] to develop smart cosmetic products and functional food,[6,14−16] and to crystallize active pharmaceutical ingredients (API) for formation of drug nanocrystals.[17,18] Therefore, an effective synthesis of nanoemulsions and better understanding of mechanisms involved in their formation are critical for use in the above applications.

Nanoemulsions are synthesized by two broad techniques: high-energy methods and low-energy methods.[1,5] High-energy methods, such as high-pressure homogenization and ultrasonication, use excess energy ($\sim 10^8$ W/kg) to break large droplets to about 100 nm in size.[19−21] Due to their brute force technique, high-energy methods provide a robust way to synthesize nanoemulsions with a dispersed phase volume fraction as high as 40%.[18,22,23] However, the use of excess shear makes them inefficient and susceptible to heat effects. In contrast, low-energy methods exploit the low interfacial tension property of a system to reduce droplet size with energy input that can be achieved by a magnetic stirrer ($\sim 10^{3−5}$ W/kg)[1,3,4] and provide an easy and scalable route to make nanoemulsions without the use of excess shear. The most widely used low-energy method in literature is the emulsion inversion point, EIP (also known as phase inversion composition), where components are mixed in a specific order at constant temperature to produce nanoemulsions.[24−26] However, there are critical gaps in the literature about the mechanism of EIP nanoemulsion synthesis, and we aim to address some of them through this paper.

The central dogma in EIP literature is that for successful synthesis of nanoemulsions, spontaneous change in interface curvature is required through change in composition.[27] Numerous studies suggest that to make O/W nanoemulsions, the continuous phase should be added to a mixture of dispersed phase and surfactant (denoted here by method B in Figure 1a).[24−26,28,29] The researchers argue that method B is effective since the system phase inverts during the process of continuous phase addition leading to extremely low interfacial tension and efficient droplet breakup.[24−26,30,31] Though this mechanism is intuitive, it ignores the effect of interaction between surfactant and the liquid phases during nanoemulsion formation. On the other hand, studies on water-in-oil (W/O) nanoemulsions use both orders of mixing to prepare nanoemulsions, i.e., dispersed phase being added to a mixture of continuous phase and surfactant (denoted here by method A in Figure 1b) as well as continuous phase being added to a mixture of dispersed phase and surfactant.[32,33] Therefore, no unifying mechanism exists to explain formation of O/W and W/O nanoemulsions, and we were motivated to investigate the mechanism in more detail.

(a)

(b)
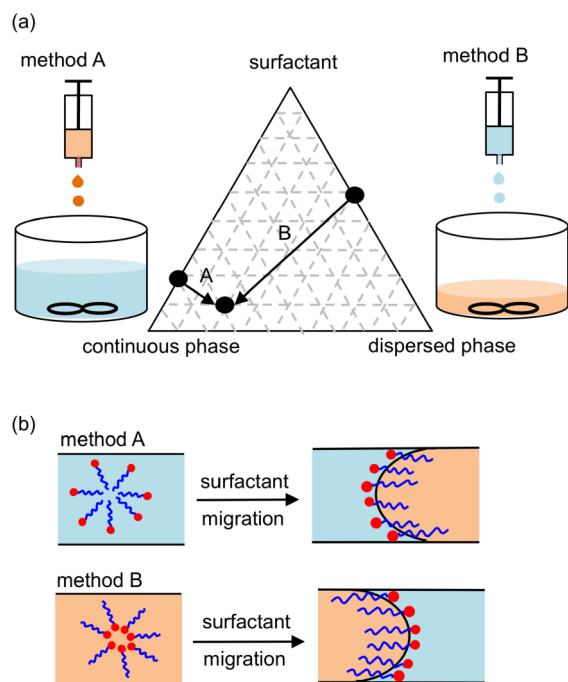
Figure 1. Proposed mechanism for low-energy nanoemulsification. (a) The order of mixing is important in the process of nanoemulsification. The two ways of mixing are adding dispersed phase in a mixture of continuous phase and surfactant (method A) and adding continuous phase in a mixture of dispersed phase and surfactant (method B). (b) For effective synthesis of nanoemulsions, migration of the emulsifier to the interface is critical. We propose that synthesis will be more effective for method A when the surfactant dislikes the continuous phase, whereas it will be more effective for method B when the surfactant dislikes the dispersed phase.

Komaiko and McClements investigated the effect of different orders of mixing and concluded that method B is able to make nanoemulsions, whereas method A fails to do so.[34] On the other hand, Anton and Vandamme showed that the diffusion of surfactant is the critical step for nanoemulsion formation but did not investigate the effect of interaction with liquid phases.[35] Forgiarini et al. hypothesized that kinetics may be important in formation of nanoemulsions but did not provide any experimental evidence for the same.[25] In this paper, we vary the interaction between surfactant and liquid phase to control the surfactant migration to the interface during nanoemulsion formation. We hypothesize that for effective transport of surfactant to the interface, the surfactant should dislike the initial phase (Figure 1b). In the case of method A, surfactant should have less affinity for continuous phase, and in the case of method B, surfactant should have less affinity for dispersed phase (Figure 1b). However, for the synthesis to be more effective, the surfactant should also be soluble/miscible to some extent in the initial phase. In other words, for effective nanoemulsion synthesis, there needs to be an optimum interaction between the surfactant and liquid phases for both method A and method B. An optimum interaction between surfactant and liquid phases might also modify surfactant migration velocity, thus improving the kinetics of nanoemulsion formation. On the basis of our hypothesis, we show that method A is also effective for O/W nanoemulsion synthesis and, in many cases, superior to method B. We are also able to explain why method A is effective for W/O nanoemulsions.[33]

To demonstrate our hypothesis, we selected a model system of decane-in-water (O/W) nanoemulsions emulsified by a mixture of nonionic surfactants (Tween 80 and Span 80). By varying the relative amount of Tween 80 and Span 80 in the surfactant mixture, we changed the HLB (hydrophilic–lypophilic balance) value of the surfactant, a parameter that estimates the affinity of surfactant toward liquid phases. The value of HLB for a mixture of Tween 80 and Span 80 can be calculated by $HLB = 4.3x + 15(1 - x)$, where x is the weight fraction of Span 80 in the mixture. A HLB value of 4.3 (pure Span 80) represents an oleophilic surfactant, whereas a HLB value of 15 (pure Tween 80) represents a hydrophilic surfactant. We prepared nanoemulsions with 15 wt % decane−15 wt % surfactant−70 wt % water (surfactant-to-oil ratio, SOR = 1; see the Supporting Information for details). An overview of our results using this composition is provided in Figure 2a. Our results demonstrate that method B synthesizes decane-in-water nanoemulsions only for HLB $\geq$ 13.0. In contrast, method A synthesizes nanoemulsions for HLB $\leq$ 13.5. The visual appearance of the nanoemulsion solutions (Figure 2a) also indicates that method B is unstable for HLB < 13.0 and method A is unstable for HLB > 13.5. This result is consistent with our anticipation, since method B is unstable for lower HLB or when the surfactant is less hydrophilic, whereas method A is unstable for higher HLB, when the surfactant is more hydrophilic. This result opens up the opportunity to potentially synthesize nanoemulsions for HLB values that are not possible with method B, the conventional method used in the literature. We also note that for both methods the average droplet size passes through a minimum with HLB, suggesting that there is an optimum interaction between the surfactant and the liquid phases that is most effective in creating small emulsion droplets.

The effectiveness of method A and method B to synthesize nanoemulsions also depends on the relative amount of dispersed phase and surfactant. We varied the surfactant-to-oil ratio by making nanoemulsions with the composition 7.5 wt % decane−22.5 wt % surfactant−70 wt % water (SOR = 3). The results are summarized in Figure 2b. We observe that the nanoemulsion droplet size for SOR = 3 is smaller than that for SOR = 1 for all samples. Further, method B is now stable for HLB = 11−15, whereas method A is only stable for HLB $\leq$ 13.5. The optimum HLB for method B has shifted to 14.3, whereas there is no observable optimal value for method A. We believe that these observations indicate that at SOR = 3 for method B the diffusion of surfactant from dispersed phase to continuous phase is sufficient to make a stable nanoemulsion even for low HLB value since the relative amount of surfactant is higher.

We also investigated the effects of the order of addition on nanoemulsion formation for a reverse nanoemulsification system, i.e., water-in-decane (W/O) nanoemulsion. We synthesized nanoemulsions with 10 wt % water−10 wt % surfactant−80 wt % decane using both methods A and B for different HLB values. We observed that method A is effective for the entire range of HLB = 4.3−9.0, whereas method B is only effective for HLB = 4.0 (Figure 2c). The limited range of method B is consistent with our hypothesis that method B works when surfactant dislikes the dispersed phase, i.e., dislikes water, or for low HLB. This result may explain the reason why previous literature has used method A to generate W/O nanoemulsions.[33]
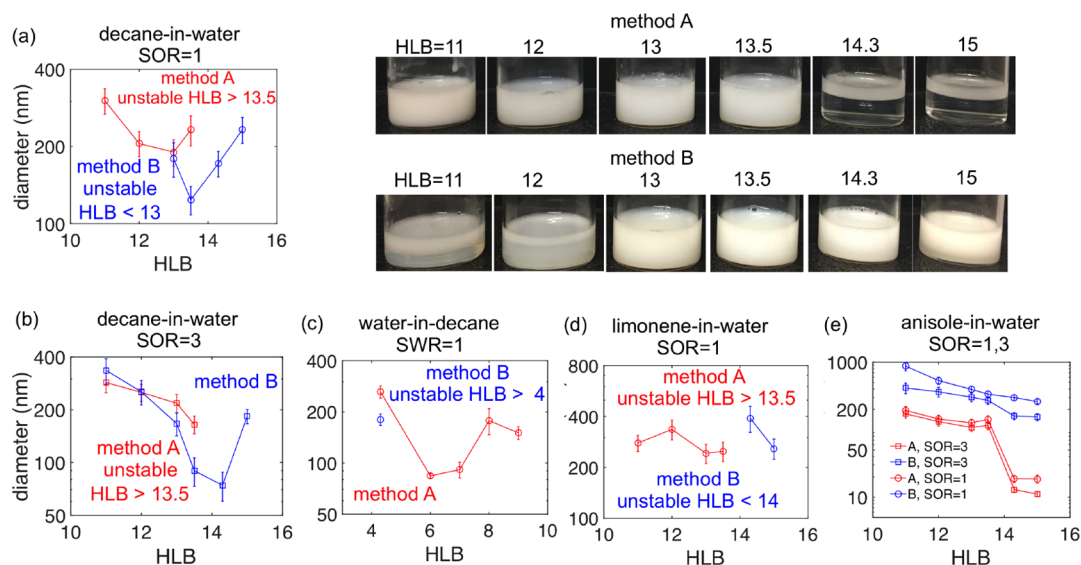
Figure 2. Demonstration of the proposed mechanism with Tween 80 and Span 80. (a) Average droplet size as a function of HLB value for 15 wt % decane−15 wt % surfactant−70 wt % water (SOR = 1) nanoemulsions. Method A is unstable for HLB > 13.5, whereas method B is unstable for HLB < 13. This can also be observed from the visual appearance of nanoemulsion solutions for different HLB values. (b) Average droplet size for 7.5 wt % decane−22.5 wt % surfactant−70 wt % (SOR = 3) nanoemulsions for both method A and method B. The trends are similar to those for SOR = 1. (c) 10 wt % water−10 wt % surfactant−80 wt % decane (surfactant-to-water ratio, SWR = 1) nanoemulsions for both method A and method B. Method B produces a nanoemulsion only for HLB = 4, whereas method A work for HLB = 4.0−9.0. Average droplet size as a function of HLB for (d) 15 wt % limonene−15 wt % surfactant−70 wt % water (SOR = 1) and (e) 15 wt % anisole−15 wt % surfactant−70 wt % water (SOR = 1) and 7.5 wt % anisole−22.5 wt % surfactant−70 wt % water (SOR = 3). The results for limonene are similar to decane for SOR = 1. The results for anisole show that method A is superior to method B for the entire HLB range. The error bars in all figures indicate the polydispersity of the samples. The HLB was varied by using a mixture of Tween 80 and Span 80.

To further support our hypothesis, we synthesized nano-emulsions using different model systems with compositions 15 wt % limonene−15 wt % surfactant−70 wt % water, 15 wt % anisole−15 wt % surfactant−70 wt % water, and 7.5 wt % anisole−22.5 wt % surfactant−70 wt % water (Figure 2d,e). We chose limonene as an oil phase because it is commonly used to prepare food-grade nanoemulsions.[29] On the other hand, anisole-in-water nanoemulsions are an attractive choice for pharmaceutical formulation and manufacturing.[17,18] Figure 2d shows that for limonene-in-water nanoemulsions, method A works better for HLB = 11.0−13.5, whereas method B works better for HLB = 14.3−15.0. These results are also consistent with our proposed explanation of nanoemulsion formation. We note that it is possible to create small droplet sizes with method A, providing a route to create smaller food-grade nano-emulsions than the ones reported in the literature. Figure 2e shows that for anisole-in-water nanoemulsions, we can obtain droplet sizes as small as 10 nm using method A. The results also indicate that the nanoemulsion droplets for SOR = 3 are smaller than those for SOR = 1, as expected. However, the trends show that both methods work for the entire HLB range. Though this result might appear to be a bit surprising at first, it is possible because anisole is a very good solvent and has a solubility of 15 mg/L in water.[36] Therefore, the surfactants have some solubility in both phases for the entire HLB range.

Lastly, to ensure that our hypothesis also works for different surfactants, we prepared nanoemulsions by using (i) Tween 85 (HLB = 11), (ii) 50 wt % Tween 85−50 wt % Tween 80 (HLB = 13), (iii) Tween 80 (HLB = 15), and (iv) Tween 40 (HLB = 15.8). We synthesized decane-in-water nanoemulsions with the composition 15 wt % oil phase−15 wt % surfactant−70 wt % water using both method A and method B. Our results are summarized in Figure 3. The results show that our hypothesis is
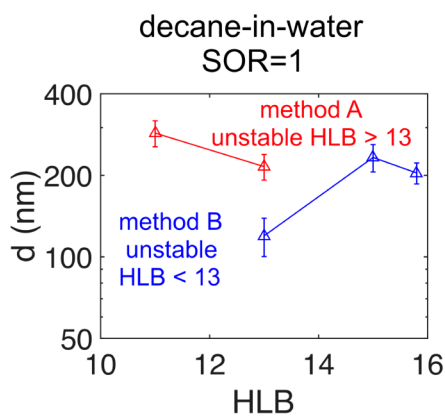
Figure 3. Demonstration of the proposed mechanism for different surfactants. Average droplet size as a function of HLB value for 15 wt % decane−15 wt % surfactant−70 wt % water (SOR = 1) nanoemulsions. Method A is unstable for HLB > 13, whereas method B is unstable for HLB < 13. The error bars indicate the polydispersity of the samples. The HLB was varied by using Tween 85 (HLB = 11), 50 wt % Tween 85−50 wt % Tween 80 (HLB = 13), Tween 80 (HLB = 15), and Tween 40 (HLB = 15.8).

valid for different surfactants, where method A is unstable for HLB > 13 and method B is unstable for HLB < 13. The results also indicate that both single and mixed surfactants are effective in nanoemulsion synthesis. Finally, the trend of average droplet size with HLB is qualitatively consistent with the results obtained in Figure 2a and thus underscores the generality of our proposed method.

Oil-in-water (O/W) nanoemulsions are commonly used in the applications of pharmaceuticals formulation and delivery.[37] Here, we demonstrate an approach using O/W-nanoemulsion-
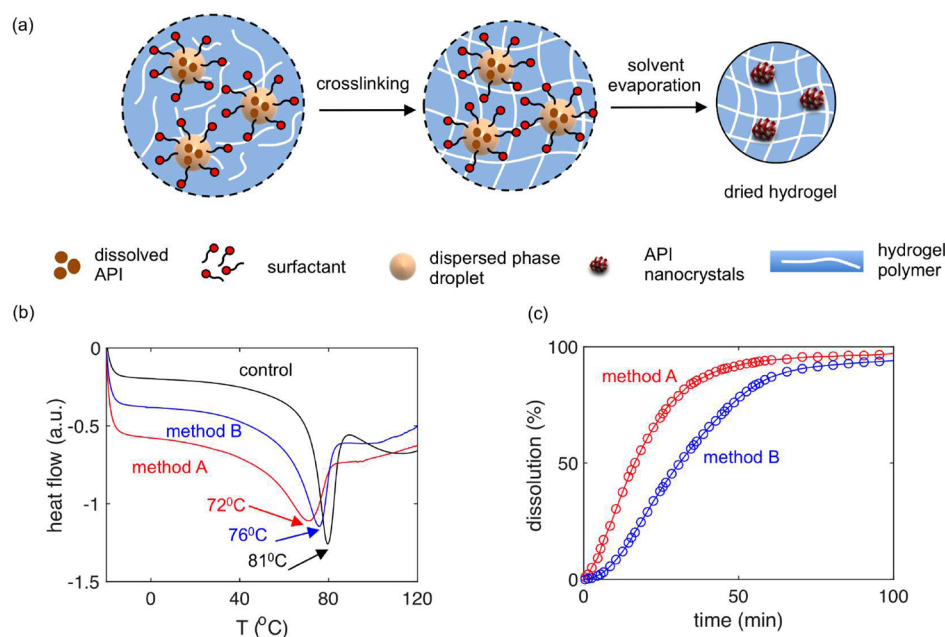
Figure 4. Application of low-energy nanoemulsions in pharmaceutical formulation. (a) Overview of the experimental procedure to make hydrophobic API nanocrystals encapsulated inside the composite hydrogels. (b) Data from differential scanning calorimetry (DSC) of dried hydrogels with API nanocrystals embedded in the polymer core matrix showing a larger decrease in the melting point of API for method A as compared to method B. (c) In vitro dissolution profiles of fenofibrate nanocrystals in composite hydrogels show a faster API release for method A as compared to method B.

laden biocompatible hydrogels to improve the dissolution kinetics and oral bioavailability of poorly water-soluble active pharmaceutical ingredients (APIs). Over the past few years, the development of hydrophobic API nanocrystals and their formulation has been a major focus of pharmaceutical research.[17,18,38,39] In this study, we generated nanocrystals of fenofibrate (a model poorly water-soluble API) embedded in an alginate hydrogel polymer matrix with controlled crystal size (Figure 4a). To do so, we prepared low-energy O/W nanoemulsions which consisted of anisole containing saturated amount of fenofibrate as the dispersed phase and 4 wt % aqueous alginate solution as the continuous phase. The composition of the nanoemulsion solution is 15 wt % oil phase−15 wt % surfactant (HLB = 12)−70 wt % alginated aqueous phase. The average nanoemulsion droplet size for method A and method B are 140 ± 20 and 530 ± 70 nm, respectively. After preparing nanoemulsions using both method A and method B, the uncrosslinked alginate nanoemulsion solutions were dripped through a syringe-needle system (30 gauge) into a 6% w/v CaCl$_2$ solution within a centrifuge, as described in our previous work[18,40] (see the Supporting Information for details). We obtain hydrogel bead sizes of 90 ± 5 μm. Ionic cross-linking of alginate creates a cross-linked polymer network, trapping the nanoemulsion droplets containing the API. Crystallization of API is induced by controlled evaporation of both the dispersed organic phase and the aqueous phase at 60 °C. In our previous work, we show that the crystal size of API is dictated by the nanoemulsion droplet size,[17,18] and thus, we expect the crystal size from method A to be lower than that from method B. This is corroborated by the differential scanning calorimetry (DSC) measurements of the fenofibrate nanocrystal encapsulated in dried hydrogel particles, which show that the melting point of the fenofibrate from method A (72 °C) is smaller than that from method B (76 °C, Figure 4b). This is consistent with the prior reports in the

literature where DSC measurements show the melting point depression in API nanocrystals (crystal size <300 nm).[41] Finally, we also see a significant improvement in drug dissolution kinetics when comparing method A and method B (Figure 4c). For an 80% dissolution of fenofibrate, method A requires about 30 min, whereas method B requires about 50 min. On the basis of the nanoemulsion droplet size measurements, we expect that the crystal sizes from method B are approximately 4 times larger than the crystals from method A.[18] This would imply that in a completely dissolution-controlled regime, the dissolution time scale in method A is 4 times faster than in method B.[17] However, the dissolution time is also affected by mass transfer through the gel matrix, which explains the less than 4-fold difference in time scales.[18]

We also exploit the understanding of W/O nanoemulsion formation using the low-energy method to fabricate nanosized hydrogels or so-called nanogels. Polymeric nanogels have attracted tremendous interest over the last several years owing to their potential for applications in pharmaceutical and biomedical fields, such as delivery systems for drugs and biomacromolecules, regenerative medicine, and bioimaging.[42,43] Here, we present a method for the fabrication of alginate nanogel particles in the size range of 200−500 nm using W/O nanoemulsions as templates. A nanoemulsion is synthesized using method A with the following composition: 10 wt % alginated aqueous phase−10 wt % surfactant−80 wt % decane. The surfactant was taken to be a mixture of Tween 80 and Span 80 with HLB = 7. The aqueous (dispersed) phase contained 1.5 wt % alginate and a cross-linking precursor, Ca−EDTA complex. We prepared the Ca−EDTA complex by mixing a solution of calcium chloride (50 mM) with a solution of disodium EDTA (100 mM). The following reaction was used to prepare the complex: CaCl$_2$ + Na$_2$H$_2$EDTA ⇌ Ca−EDTA + 2NaCl + 2H$^+$ (see the Supporting Information for details). Disodium-EDTA was used in excess to avoid the formation of

$CaCl_2$, which could cause the pregelation of alginate aqueous phase. Once we synthesized the nanoemulsions, acetic acid was introduced into the solution, which triggered the dissociation of Ca−EDTA complex, resulting in the release of Ca^{2+} ions from the complex[44] and the cross-linking of the aqueous alginate nanodroplets to yield the alginate nanoparticles (Figure 5a).
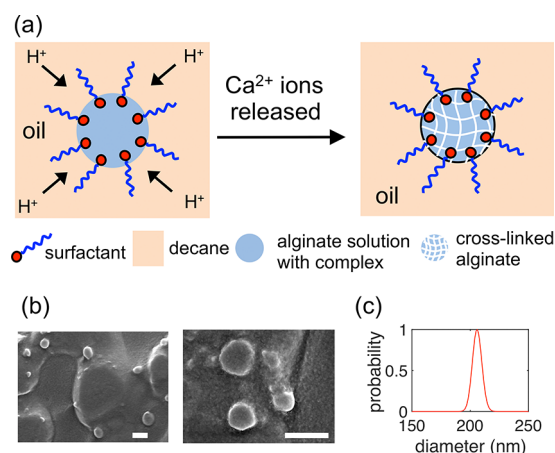
Figure 5. Synthesis of biocompatible soft nanogel materials using W/O nanoemulsions as templates. (a) Nanoemulsions with 1.5 wt % alginate and 50 mM Ca−EDTA complex in water as dispersed phase and decane as continuous phase were prepared by method A. Once the nanoemulsions were prepared, acetic acid is introduced into the nanoemulsion solution to cross-link the alginate nanodroplets. Cross-linking is induced since acetic acid releases the Ca^{2+} ions from the water-soluble Ca−EDTA complex. (b) High-resolution SEM images of alginate nanoparticles. The scale bar is 300 nm for both images. (c, bottom right) Size distribution of hydrated alginate nanogel particles measured by dynamic light scattering (DLS).

The resultant nanogel particles were then separated from the decane phase using centrifugation and resuspended in water. The high-resolution SEM image of the dried alginate particles (Figure 5b) and the size distribution measured by the dynamic light scattering (DLS) technique (Figure 5c) confirm the successful synthesis of alginate hydrogels in the nanoscale range. In addition, DLS measurement of alginate nanogel suspensions (Figure 5c) indicates that the size of nanogels is nearly identical to that of the parent nanoemulsion (∼220 nm), demonstrating the successful templating of uniform alginate hydrogel nanoparticles from W/O nanoemulsions. To the best of our knowledge, this is the first demonstration of fabrication of alginate nanogel particles using a low-energy nanoemulsion as a template. These nanogels are good candidates for use in biomedical applications due to their nature and size. Our approach to prepare nanogels does not require significant energy input when compared to any state-of-the-art techniques (e.g., microfluidics, centrifugal microfluidics)[45,46] and can be performed using only a magnetic stirrer in a batch process. This makes our method attractive for scale up and high-throughput synthesis. Moreover, our technique is highly flexible in that we can tune parameters such as concentration of alginate and water weight fraction to prepare nanoparticles with throughput as high as 200 μg/mL.

In this paper, we showed that surfactant interactions with liquid phases will dictate the order of mixing for successful nanoemulsion synthesis. We believe that the proposed mechanism of formation for both O/W and W/O nano-emulsions has great implications in the field of nanotechnology,

as it opens up a range of possibilities to the already existing applications. For instance, we demonstrated superior synthesis of food-grade nanoemulsions; effective formulation for pharmaceutical, nutritional, and nutriceutical materials; and even synthesis of biocompatible polymeric soft nanomaterials (i.e., alginate nanogels). Future studies could focus on generation of double nanoemulsions using low-energy methods, since the order-of-mixing in both O/W and W/O nanoemulsion formation can now be tuned to our advantage. In addition, biological applications, such as in vivo experiments and bioimaging, can be explored through investigations in the synthesis of hydrogels in the nanosize range using a low-energy nanoemulsion as a template. We hope that this paper will be useful for researchers working with nanoemulsions by providing them with a rationale for the design of low-energy methods.

■ ASSOCIATED CONTENT

Ⓢ Supporting Information
The Supporting Information is available free of charge on the ACS Publications website at DOI: 10.1021/acs.langmuir.7b01104.

■ AUTHOR INFORMATION

Corresponding Author
*E-mail: pdoyle@mit.edu.

ORCID Ⓞ
Ankur Gupta: 0000-0003-3474-9522
Patrick S. Doyle: 0000-0003-2147-9172

Author Contributions
[†]A.G. and A.Z.M.B. contributed equally to this work.

Notes
The authors declare no competing financial interest.

■ ACKNOWLEDGMENTS

■ REFERENCES

(1) Gupta, A.; Eral, H. B.; Hatton, T. A.; Doyle, P. S. Nanoemulsions: formation, properties and applications. *Soft Matter* **2016**, *12*, 2826−2841.
(2) Mason, T. G.; Wilking, J.; Meleson, K.; Chang, C.; Graves, S. Nanoemulsions: formation, structure, and physical properties. *J. Phys.: Condens. Matter* **2006**, *18*, R635.
(3) Tadros, T.; Izquierdo, P.; Esquena, J.; Solans, C. Formation and stability of nano-emulsions. *Adv. Colloid Interface Sci.* **2004**, *108-109*, 303−318.
(4) Solans, C.; Izquierdo, P.; Nolla, J.; Azemar, N.; Garcia-Celma, M. Nano-emulsions. *Curr. Opin. Colloid Interface Sci.* **2005**, *10*, 102−110.
(5) Fryd, M. M.; Mason, T. G. Advanced nanoemulsions. *Annu. Rev. Phys. Chem.* **2012**, *63*, 493−518.

(6) McClements, D. J. Edible nanoemulsions: fabrication, properties, and functional performance. *Soft Matter* **2011**, 7, 2297−2316.

(7) Kumar, M.; Misra, A.; Babbar, A.; Mishra, A.; Mishra, P.; Pathak, K. Intranasal nanoemulsion based brain targeting drug delivery system of risperidone. *Int. J. Pharm.* **2008**, 358, 285−291.

(8) Sarker, D. K. Engineering of nanoemulsions for drug delivery. *Curr. Drug Delivery* **2005**, 2, 297−310.

(9) Lovelyn, C.; Attama, A. A. Current state of nanoemulsions in drug delivery. *J. Biomater. Nanobiotechnol.* **2011**, 2, 626.

(10) Shakeel, F.; Baboota, S.; Ahuja, A.; Ali, J.; Aqil, M.; Shafiq, S. Nanoemulsions as vehicles for transdermal delivery of aceclofenac. *AAPS PharmSciTech* **2007**, 8, 191−199.

(11) Anton, N.; Benoit, J.-P.; Saulnier, P. Design and production of nanoparticles formulated from nano-emulsion templatesa review. *J. Controlled Release* **2008**, 128, 185−199.

(12) Landfester, K. Miniemulsion polymerization and the structure of polymer and hybrid nanoparticles. *Angew. Chem., Int. Ed.* **2009**, 48, 4488−4507.

(13) Asua, J. M. Miniemulsion polymerization. *Prog. Polym. Sci.* **2002**, 27, 1283−1346.

(14) McClements, D. J.; Rao, J. Food-grade nanoemulsions: formulation, fabrication, properties, performance, biological fate, and potential toxicity. *Crit. Rev. Food Sci. Nutr.* **2011**, 51, 285−330.

(15) Rao, J.; McClements, D. J. Food-grade microemulsions, nanoemulsions and emulsions: fabrication from sucrose monopalmitate & lemon oil. *Food Hydrocolloids* **2011**, 25, 1413−1423.

(16) Sonneville-Aubrun, O.; Simonnet, J.-T.; L'Alloret, F. Nano-emulsions: a new vehicle for skincare products. *Adv. Colloid Interface Sci.* **2004**, 108-109, 145−149.

(17) Eral, H. B.; O'Mahony, M.; Shaw, R.; Trout, B. L.; Myerson, A. S.; Doyle, P. S. Composite Hydrogels Laden with Crystalline Active Pharmaceutical Ingredients of Controlled Size and Loading. *Chem. Mater.* **2014**, 26, 6213−6220.

(18) Badruddoza, A. Z. M.; Godfrin, P. D.; Myerson, A. S.; Trout, B. L.; Doyle, P. S. Core−Shell Composite Hydrogels for Controlled Nanocrystal Formation and Release of Hydrophobic Active Pharmaceutical Ingredients. *Adv. Healthcare Mater.* **2016**, 5, 1960−1968.

(19) Gupta, A.; Eral, H. B.; Hatton, T. A.; Doyle, P. S. Controlling and predicting droplet size of nanoemulsions: scaling relations with experimental validation. *Soft Matter* **2016**, 12, 1452−1458.

(20) Gupta, A.; Narsimhan, V.; Hatton, T. A.; Doyle, P. S. Kinetics of the Change in Droplet Size during Nanoemulsion Formation. *Langmuir* **2016**, 32, 11551−11559.

(21) Delmas, T.; Piraux, H.; Couffin, A.-C.; Texier, I.; Vinet, F.; Poulin, P.; Cates, M. E.; Bibette, J. How to prepare and stabilize very small nanoemulsions. *Langmuir* **2011**, 27, 1683−1692.

(22) Wilking, J. N.; Mason, T. G. Irreversible shear-induced vitrification of droplets into elastic nanoemulsions by extreme rupturing. *Phys. Rev. E* **2007**, 75, 041407.

(23) Helgeson, M. E.; Moran, S. E.; An, H. Z.; Doyle, P. S. Mesoporous organohydrogels from thermogelling photocrosslinkable nanoemulsions. *Nat. Mater.* **2012**, 11, 344−352.

(24) Forgiarini, A.; Esquena, J.; González, C.; Solans, C. Studies of the relation between phase behavior and emulsification methods with nanoemulsion formation. In *Trends in Colloid and Interface Science XIV*; Progress in Colloid and Polymer Science; Buckin, V., Ed.; Springer, 2000; Vol. 115, pp 36−39, doi: 10.1007/3-540-46545-6_8.

(25) Forgiarini, A.; Esquena, J.; Gonzalez, C.; Solans, C. Formation of nano-emulsions by low-energy emulsification methods at constant temperature. *Langmuir* **2001**, 17, 2076−2083.

(26) Forgiarini, A.; Esquena, J.; González, C.; Solans, C. Formation and stability of nano-emulsions in mixed nonionic surfactant systems. In *Trends in Colloid and Interface Science XV*; Progress in Colloid and Polymer Science; Koutsoukos, P. G., Ed.; Springer, 2001; Vol. 118, pp 184−189, doi: 10.1007/3-540-45725-9_42.

(27) Roger, K.; Cabane, B.; Olsson, U. Emulsification through surfactant hydration: the PIC process revisited. *Langmuir* **2011**, 27, 604−611.

(28) Fernandez, P.; André, V.; Rieger, J.; Kühnle, A. Nano-emulsion formation by emulsion phase inversion. *Colloids Surf., A* **2004**, 251, 53−58.

(29) Ostertag, F.; Weiss, J.; McClements, D. J. Low-energy formation of edible nanoemulsions: factors influencing droplet size produced by emulsion phase inversion. *J. Colloid Interface Sci.* **2012**, 388, 95−102.

(30) Maestro, A.; Solè, I.; González, C.; Solans, C.; Gutiérrez, J. M. Influence of the phase behavior on the properties of ionic nanoemulsions prepared by the phase inversion composition method. *J. Colloid Interface Sci.* **2008**, 327, 433−439.

(31) Anton, N.; Vandamme, T. F. Nano-emulsions and micro-emulsions: clarifications of the critical differences. *Pharm. Res.* **2011**, 28, 978−985.

(32) Uson, N.; Garcia, M. J.; Solans, C. Formation of water-in-oil (W/O) nano-emulsions in a water/mixed non-ionic surfactant/oil systems prepared by a low-energy emulsification method. *Colloids Surf., A* **2004**, 250, 415−421.

(33) Porras, M.; Solans, C.; Gonzalez, C.; Gutiérrez, J. Properties of water-in-oil (W/O) nano-emulsions prepared by a low-energy emulsification method. *Colloids Surf., A* **2008**, 324, 181−188.

(34) Komaiko, J.; McClements, D. J. Optimization of isothermal low-energy nanoemulsion formation: Hydrocarbon oil, non-ionic surfactant, and water systems. *J. Colloid Interface Sci.* **2014**, 425, 59−66.

(35) Anton, N.; Vandamme, T. F. The universality of low-energy nano-emulsification. *Int. J. Pharm.* **2009**, 377, 142−147.

(36) Chiou, C. T.; Porter, P. E.; Schmedding, D. W. Partition equilibriums of nonionic organic compounds between soil organic matter and water. *Environ. Sci. Technol.* **1983**, 17, 227−231.

(37) Chen, H.; Khemtong, C.; Yang, X.; Chang, X.; Gao, J. Nanonization strategies for poorly water-soluble drugs. *Drug Discovery Today* **2011**, 16, 354−360.

(38) Shegokar, R.; Müller, R. H. Nanocrystals: industrially feasible multifunctional formulation technology for poorly soluble actives. *Int. J. Pharm.* **2010**, 399, 129−139.

(39) Gao, L.; Zhang, D.; Chen, M. Drug nanocrystals for the formulation of poorly soluble drugs and its application as a potential drug delivery system. *J. Nanopart. Res.* **2008**, 10, 845−862.

(40) Eral, H. B.; Safai, E. R.; Keshavarz, B.; Kim, J. J.; Lee, J.; Doyle, P. S. Governing principles of alginate microparticle synthesis with centrifugal forces. *Langmuir* **2016**, 32, 7198−7209.

(41) Dwyer, L.; Michaelis, V.; O'Mahony, M.; Griffin, R.; Myerson, A. Confined crystallization of fenofibrate in nanoporous silica. *CrystEngComm* **2015**, 17, 7922−7929.

(42) Sasaki, Y.; Akiyoshi, K. Nanogel engineering for new nanobiomaterials: from chaperoning engineering to biomedical applications. *Chem. Rec.* **2010**, 10, 366−376.

(43) Kabanov, A. V.; Vinogradov, S. V. Nanogels as pharmaceutical carriers: finite networks of infinite capabilities. *Angew. Chem., Int. Ed.* **2009**, 48, 5418−5429.

(44) Utech, S.; Prodanovic, R.; Mao, A. S.; Ostafe, R.; Mooney, D. J.; Weitz, D. A. Microfluidic generation of monodisperse, structurally homogeneous alginate microgels for cell encapsulation and 3D cell culture. *Adv. Healthcare Mater.* **2015**, 4, 1628−1633.

(45) Liu, M.; Sun, X.-T.; Yang, C.-G.; Xu, Z.-R. On-chip preparation of calcium alginate particles based on droplet templates formed by using a centrifugal microfluidic technique. *J. Colloid Interface Sci.* **2016**, 466, 20−27.

(46) Mazutis, L.; Vasiliauskas, R.; Weitz, D. A. Microfluidic production of alginate hydrogel particles for antibody encapsulation and release. *Macromol. Biosci.* **2015**, 15, 1641−1646.